Agricultural and Forest Meteorology 279 (2019) 107666

Contents lists available at ScienceDirect

Agricultural and Forest Meteorology

journal homepage: www.elsevier.com/locate/agrformet

Testing an energy exchange and microclimate cooling hypothesis for the effect of vegetation configuration on urban heat

Jingli Yan[a], Weiqi Zhou[b,c], G. Darrel Jenerette[a,*]

[a] Department of Botany and Plant Sciences, University of California Riverside, Riverside, CA 92521, USA
[b] State Key Laboratory of Urban and Regional Ecology, Research Center for Eco-Environmental Sciences, Chinese Academy of Sciences, No. 18 Shuangqing Road, Beijing 100085, China
[c] University of Chinese Academy of Sciences, No. 19 Yuquan Road, Beijing 100049, China

ARTICLE INFO

Keywords:
Configuration
Scale
Urban
Microclimate
MASTER
Remote sensing
Vegetation

ABSTRACT

While an effect of urban vegetation configuration on land surface temperature (LST) has been identified worldwide, the mechanism underlying configuration-LST relationships remains unclear as most urban LST data only resolve to neighborhood scales. Here we ask: does urban vegetation provide more cooling arranged in fewer and larger patches or more numerous but smaller patches in the Phoenix metropolitan area, Arizona, USA? We hypothesized the combination of energy exchanges between adjacent patches and microclimate cooling induced by vegetation are key processes determining how configuration affects LST. Using high resolution thermal data (7 m), we evaluated predictions from this hypothesis through a multiple scale analysis spanning from within individual patches to among neighborhoods. We found tree cover is the dominant factor influencing urban cooling and that tree and grass configurations also substantially affect cooling, with effects generally exceeding 40% that of tree cover. The effects of tree and grass cover and configuration on LST were scale-dependent and reflect differences from within individual patches to among neighborhoods. In general, greater edge density and shape complexities of vegetation patches cool the landscape but may warm individual vegetation patches. Conversely, increasing individual vegetation patch size and reducing shape complexity may lead to cooler vegetation patches but a hotter landscape. Our findings suggest more edge area strengthens energy exchanges between vegetation and surroundings and more vegetation core area lead to greater cooling within individual patches. Through applications of high resolution thermal remote sensing, we are able to more directly connect effects of land cover composition and configuration to LST distributions that can help cities plan and evaluate local climate adaptation strategies.

1. Introduction

Mitigating urban heat is increasingly valued for decreasing human health vulnerabilities and energy use (Peng et al., 2018; Jenerette, 2018; McDonald et al., 2019). Green infrastructure (GI), including green roofs and urban greenspace, provides urban cooling of both air and land surface temperatures (LST), through shading, higher evapotranspiration rates, and lower emissivity than built structures (Bowler et al., 2010; Weng et al., 2004). While vegetation cooling effects are widespread, the magnitude of vegetation cooling varies dramatically both among and within cities throughout the world (Kong et al., 2014; Li et al., 2012; Skelhorn et al., 2014; Tayyebi and Jenerette, 2016; Shiflett et al., 2017). Vegetation configuration, or spatial pattern, has been identified as a prominent factor contributing to variation in urban cooling benefits (Fan et al., 2015; Kong et al., 2014; Li et al., 2013; Yan et al., 2018; Myint et al., 2015; Zhou et al., 2011, 2017). While configuration effects are generally more limited in the magnitude of cooling than the effects of vegetation density, configuration can have prominent effects in cities such as Phoenix, AZ (Li et al., 2016) and Sacramento, CA (Zhou et al., 2017). However, configuration effects are varied in the direction of effect: increasing landscape fragmentation is in some cases associated with greater cooling (Zhou et al., 2011; Li et al., 2011; Fan et al., 2015) while in other cases greater warming (Zhang et al., 2009; Connors et al., 2012). Differences in urban climate responses to vegetation configuration suggest large uncertainties remain in identifying the mechanisms underlying how configuration affects LST. Because of these uncertainties, at present we can't answer a seemingly straightforward question: does urban vegetation provide more cooling arranged in fewer and larger patches or more numerous but smaller patches?

* Corresponding author.
E-mail address: darrel.jenerette@ucr.edu (G.D. Jenerette).

https://doi.org/10.1016/j.agrformet.2019.107666
Received 5 March 2019; Received in revised form 31 May 2019; Accepted 17 July 2019
Available online 24 August 2019
0168-1923/

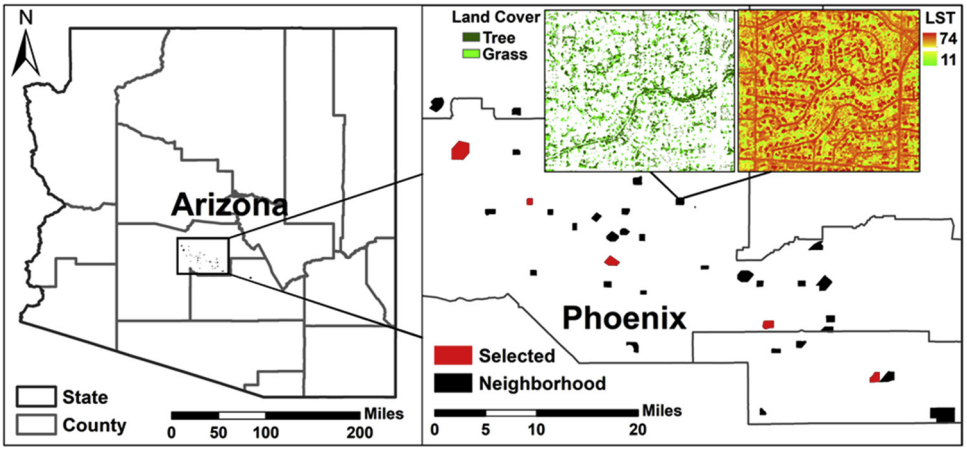

Fig. 1. The neighborhoods and associated Land Cover/LST map located in Phoenix metropolitan area of Arizona.

As a working hypothesis to explain the effects of vegetation configuration on urban temperatures we consider two processes, energy exchanges across patch edges and microclimate cooling within vegetated patch core areas, may be simultaneously influencing the role of vegetation configuration on LST and contributing to uncertainty in its effects. Vegetation patches often exhibit intra-patch differences between a central core area that is relatively stable and the edge areas that are affected by the surrounding environment (Jiao et al., 2017; Laurance and Yensen, 1991). Energy exchanges between vegetation and adjacent patches can influence microclimates both within vegetated and non-vegetated patches. Proceeding from the edge to the interior of a vegetation patch, research in forests have found increasing effects of vegetation microclimate, which leads to cooler temperature within the vegetated core (Matlack, 1994). Similarly, residential areas adjacent to rice paddies had reduced air temperatures that increased non-linearly with distance into the residential patch (Yokohari et al., 2001). Although less frequently evaluated, edges are also locations where vegetation cooling effects may propagate into the neighboring built patches and potentially cool the larger landscape. Larger but fewer vegetation patches may lead to cooler vegetation but the remaining landscape is warmer because of fewer vegetation edges for energy exchanges. In contrast, more numerous but smaller vegetation patches may lead to warmer vegetation but a cooler remaining landscape because of reduced microclimate cooling but increased exchanges of energy with adjacent patches. The combination of energy exchange and microclimate cooling processes may be stronger in tree than grass dominated patches as shading by trees may induce larger cooling effects than transpiration alone.

Implicit in energy exchange and microclimate cooling effects is recognition that scale affects vegetation configuration influences on LST. Research into scaling effects has been limited by the moderate resolution of most LST data: LST pixel sizes typically range from 90 m, Landsat data, to 1 km, MODIS data. Within a city, moderate resolution LST data includes extensively mixed land covers and extensive edges between patches within individual pixels. Energy flows between patches within a single moderate resolution pixel may confound the evaluation of temperature effects at scales where urban land cover variability occurs (Zhou et al., 2011). In some studies, multiple-scale research has been achieved by upscaling or downscaling the original moderate resolution LST data (Li et al., 2013; Song et al., 2014; Weng et al., 2008, 2004; Weng and Quattrochi, 2006; Zhou et al., 2017). These findings have shown increasing scale can increase correlations between LST and vegetation density (Song et al., 2014; Fan et al., 2015; Zhou et al., 2017). Correlations between LST and some configuration metrics can show a peaked response at intermediate scales (Kong et al., 2014; Weng, 2009; Weng et al., 2008). In addition, for one metric, such as patch density, the magnitudes of correlations and even the directions of correlation may differs among studies (Zhang et al., 2009; Li et al., 2013). Although high resolution urban LST data are increasingly becoming available (Leuzinger et al., 2010; Jenerette et al., 2016), few studies have been conducted with thermal resolution less than 90 m, which restricts a fine-scale evaluation of thermal distributions (Coutts et al., 2016). Hence, evaluating micro-scale LST-vegetation interaction with both fine resolution land cover and LST data has been noted as an important research goal for improved understanding of the biophysical causes to urban heat vulnerability (Deng and Wu, 2013; Jenerette et al., 2016; Song et al., 2014; Zhang et al., 2013). With these contrasting results, more comprehensive studies of urban configuration at finer scales are needed to improve models of landscape pattern and climate relationships.

To address uncertainties in vegetation configuration effects along with changing scales on urban climate distributions, we asked: how does vegetation configuration affect urban LST from scales within an individual vegetation patch to the entire residential neighborhood? We answer this question using new analyses of existing high resolution airborne LST (7 m) and NAIP vegetation cover (1 m) data sets collected from Phoenix, AZ, USA. Phoenix serves as a hot and dry climate endpoint that can be used as a model for high temperature urbanization. We tested predictions from the energy exchange and microclimate cooling hypotheses that 1) more edges and shape complexities of vegetation landscape reduce landscape LST because it promotes energy exchange between cooler vegetation and hotter impervious surface, and that 2) within vegetation patches a gradient of temperatures will reflect warmer edges and cooler vegetation interiors. We evaluated these predictions across multiple scales ranging from within an individual vegetation patch to across a network of neighborhoods. The results provide a needed foundation for linking fine scale vegetation-LST interactions to broader scales and provide useful information for planning green infrastructure for improved urban climate resilience.

2. Study area and datasets

2.1. Study area

The Phoenix metropolitan area (centered at 33° 24′20″N, 112° 5′17″W) of Arizona, USA (Fig. 1) is a well-studied urban ecological and climate system (Chow et al., 2012; Grimm and Redman, 2004). Phoenix is located in a subtropical desert climate (Köppen Climate Classification, 1884), and features substantial variation in vegetation and built-up areas associated with residential dwellings. Historically, there are 107 days annually with a high air temperature of at least 38 °C and the number of these high temperature days are increasing (Ruddell et al., 2013). With a rapidly expanding population of approximately 4.6 million residents in 2015 (Jenerette and Wu, 2001), the region has one

of the fastest growing urban heat islands in the United States (Stone et al., 2012). As a high temperature arid site with rapid population growth, Phoenix serves a model system near an endpoint of climate conditions.

Our analysis used a sample of 35 neighborhoods from Phoenix Area Social Survey (PASS) of 2011 stratified by location (urban, suburban, fringe) and median household income (Jenerette et al., 2016). The PASS neighborhoods were selected mostly from ongoing long-term monitoring sites in Phoenix metropolitan area (Grimm and Redman, 2004), and the boundaries of PASS neighborhoods were defined using U.S. Census Bureau block groups (https://www.census.gov/geo/maps-data/data/tiger-cart-boundary.html). The neighborhoods are a physical space following census derived boundaries. The selected 35 neighborhoods with total area ranging from 55.1 to 711.5 ha, and from 6.6 to 40% vegetation percentage, and from 44.5 to 55.1 °C mean LST (Fig. 1).

2.2. Data sets

2.2.1. NAIP-based land cover map

A land cover map for this study was derived from National Agriculture Imagery Program (NAIP) imagery (Li et al., 2014). NAIP acquires aerial imagery during the agricultural growing seasons in the continental U.S. at a 1 m ground sample distance (GSD) with a horizontal accuracy that matches within six meters of photo-identifiable ground control points, which are used during image inspection. 90% of the NAIP data used in our study were acquired from June 2010, and the remainder from August to September 2010, with four multiple spectral bands at a spatial resolution of 1 m. In comparing these data with thermal data collected in 2011, we expected limited change from 2010 and 2011 as all neighborhoods had been developed for more than a decade. The classification followed the object-based classification approach (Baatz et al., 2008; Benz et al., 2004) in eCognition Developer (http://www.ecognition.com/suite/ecognition-developer), which employed an expert knowledge decision ruleset and incorporates the cadastral GIS vector layer as auxiliary data. The NAIP imagery were classified into 13 land cover/use classes with the classification overall accuracy of 92% and a kappa statistic of 0.91, and more details can be found in Li et al. (2014). Since one of our objectives is to quantify the differences of cooling effects of trees and grass, we merged tree, shrub and orchard into the new tree class, and grass and farmland were combined into the new grass class based on existing classes of Li et al. (2014) for further analysis (Fig. 1).

2.2.2. Land surface temperature

Daytime airborne LST data were derived from the MODIS/ASTER Airborne Simulator (MASTER) data. The whole Phoenix metropolitan collection campaign was conducted during July 12–13 in 2011 (Jenerette et al., 2016) with data collected from the selected neighborhoods for our analysis in the late morning from 10 am to 12 pm of July 12. During the campaign, the instrument was mounted on a Beechcraft B-200 aircraft and flew 18 tract lines in two days to obtain high spatial resolution data in Phoenix metropolitan area. The MASTER sensor acquires data over the visible through mid-infrared wavelengths (0.46–12.82 μm) in 50 spectral bands (Hook et al., 2001) with spatial resolution at approximately 7 m/pixel. A stable weather pattern prevailed during the week of July 12 that enabled the collection from an approximate uniform meteorological condition. During this campaign period, mean daily maximum air temperature was 40.1 °C and differed less than 1.3 °C, and two weather stations in study area indicate the maximum wind speed was about 4 m/s with no detected wind gust during sampling days. A temperature trend in land surfaces from beginning to end of data collection was not observed–we expect the three dimensional surface properties had much larger influence than the time within our sampling period. Likely overlapping images may help in future for better temporal correction (Tayyebi and Jenerette, 2018).

MASTER data were acquired from (http://masterprojects.jpl.nasa.gov/L2_Products), which had been initially post-processed to level 2B. ENVI/IDL was used to perform all processing of the MASTER data. Atmospheric correction of the mid-infrared wavelength data was accomplished using an in-scene atmospheric compensation technique (Johnson and Young, 1998) to obtain apparent surface reflectance, temperature, and emissivity. An emissivity normalization approach (Kealy and Hook, 1993) was used to obtain LST from the MASTER data that used multiple thermal bands to calculate both the temperature and emissivity of each pixel. Atmospheric correction of the visible through shortwave infrared wavelength data was accomplished using the quick atmospheric correction (QUAC) algorithm (Bernstein et al., 2005) within ENVI/IDL.

The geometric match between data layers is critical for analysis of high resolution data sets and a subsequent geocorrection of LST layers using the land cover map as a reference was conducted in ENVI/IDL. 50–100 pairs of points were selected according to the size of neighborhoods and allowing RMS within 0.5. Three neighborhoods failed to meet the requirement of RMS < 0.5 after several geometrical correction attempts; these neighborhoods were excluded for all analyses. After geocorrection, the spatial resolution of LST layer was resampled to 1 m to be consistent with that of NAIP land cover data (Fig. 1). More details on LST calculation can be found in Jenerette et al. (2016).

3. Analysis

While many factors affect the distribution of urban LST, our work here focused on evaluating vegetation configuration effects to LST at multiple scales. Throughout all analyses trees and grass patches were evaluated separately. We employed four landscape metrics to quantify vegetation configuration and/or spatial pattern. Three LST indices, Mean LST (Mean LST), Maximum LST (Max LST), and Minimum LST (Min LST), were calculated at each scale and/or analytical unit. Finally, we conducted Pearson correlation analysis and multiple regression analysis to explore the effects of vegetation configuration on LST, and also the scale relations of the effects.

3.1. Multiple scales approach

We conducted the analysis at three scales: neighborhood, circular plot, and patch (Fig. 2). The circular plot scale included seven different sizes of circular plots used to generate a scaling assessment. This multiple-scale approach was meant to explicitly examine the role of spatial structure. A total of 35 neighborhoods selected from PASS boundaries were deployed at the neighborhood level. For scaling assessments, we selected a subset of five neighborhoods from the 35 neighborhoods for plot-scale analysis based on three criteria. First, we selected neighborhoods large enough to allow spatial sub-sampling (Fig. 1). Second, neighborhoods that spanned the range of mean LST and vegetation cover among the 35 neighborhoods. Third, the selected neighborhoods were spatially distributed across the entire metropolitan area. To evaluate scaling relationships, seven different plot sizes (25, 40, 60, 90, 150, 200, 250 m) were selected for a scale gradient at circular plot scale. The plot sizes were selected to correspond with (or adjusted from) the spatial resolution of multispectral/thermal bands of common remote sensing products, e.g. high altitude AVIRIS (20 m), Landsat multispectral bands (30 m), planned HyspIRI (60 m), ASTER thermal infrared (90 m), Landsat-5 thermal infrared (120 m), and MODIS infrared (250 m). 100 plots for each plot size and total 700 circular plots were randomly generated in each neighborhood. The random points and multiple plot sizes were created using Arcmap 10.4 (ESRI, Redlands, CA). For each plot size, 500 circular plots and 3500 circular plots in total for five selected neighborhoods were analyzed. For patch level, all individual vegetation patches in the five selected neighborhoods were first included, then patches smaller than one pixel (approximately 1 m^2) were excluded from further analysis leaving 53,673 tree patches and 32,030 grass patches remaining for further analysis.

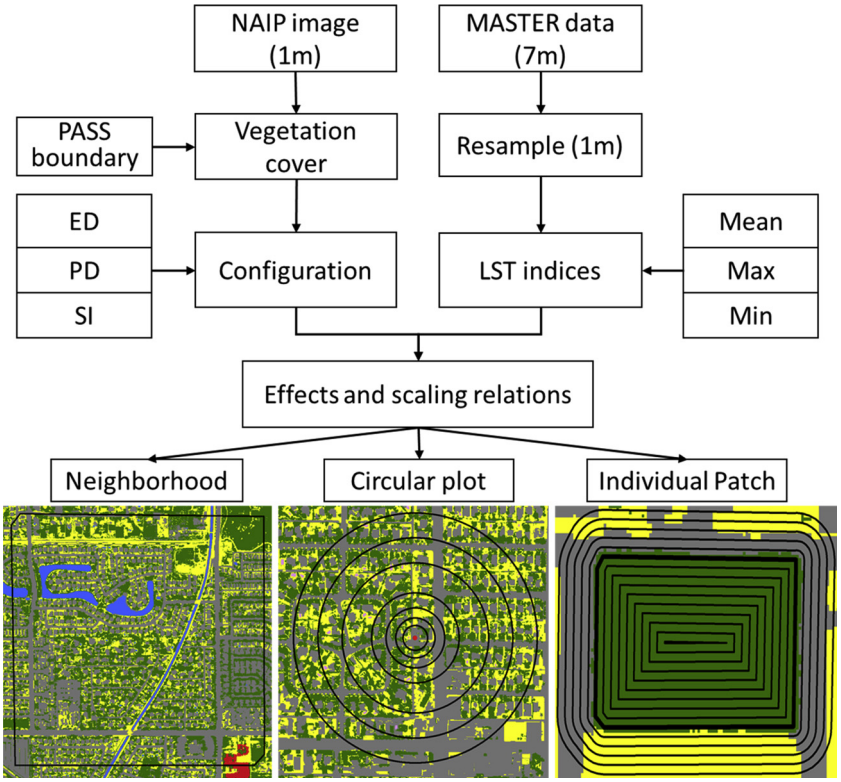

Fig. 2. The conceptual diagram of analysis. *The gray is impervious surface, yellow is bare soil, and dark green is vegetation* (For interpretation of the references to colour in this figure legend, the reader is referred to the web version of this article).

For intra-patch evaluation, buffer rings extending from the surroundings into the center of a vegetated patch were constructed to directly evaluate the edge effect of vegetation patches on microclimate distributions. To ensure high quality patches we first filtered patches with patch size larger than 500 m^2, regular shape, and homogeneous in vegetation coverage throughout. The size filter was applied to ensure the selected vegetation patches were large enough to allow generation of sufficient rings for each patch. A shape filter was used to obtain similar number of rings within a patch. With these restrictions we identified eight tree patches and five grass patches. For these patches, we created multiple buffer rings at interval of 3 m (3 resampled pixels) at both directions of the patch edges in ArcMap 10.4 (Fig. 2). We extended the buffers to include five outer rings surrounding each vegetation patch. Because of size differences, each patch has different number (11–27) of buffer rings.

3.2. Configuration metrics

At the neighborhood and circular plot scales we quantified four landscape metrics separately for tree and grass within the different analytical units. The selected four landscape metrics included one composition metric, Proportion of Vegetation Cover (VC), and three configuration metrics, Edge Density (ED), Shape Index (SI), and Patch density (PD), to represent edge, shape, and spatial pattern of vegetation landscape (Table 1). The four metrics have been used to evaluate landscape configuration in previous analyses of urban LST (Chen et al., 2014; Fan et al., 2015; Kong et al., 2014; Li et al., 2013; Myint et al., 2015; Zhou et al., 2011).

Landscape metrics were calculated in Fragstats 4.3 (https://www.umass.edu/landeco/research/fragstats/fragstats.html). First, the vegetation cover map was extracted by neighborhood and circular plot boundaries from 1 m spatial resolution NAIP-derived vegetation map in ENVI/IDL 5.3. Raster data were converted to a thematic image and were batch processed in Fragstats 4.3. Finally, landscape metrics were calculated at neighborhood and circular plot scales and exported for further statistical analysis. These statistics were designed to exemplify the mechanism of vegetation configuration impacting LST. The thematic vegetation cover map was used to calculate each of these metrics at the patch level in Fragstats 4.3.

3.3. Statistical analysis

Pearson correlation and regression analyses were used to examine the relationships between vegetation and LST indices. In the correlation analysis, trees and grass were separated from vegetation. Four vegetation indices (cover and three configuration metrics in Table 1) and three LST indices (Mean, Max, and Min) were input as variables for each vegetation types. For regression analyses, we compared linear and

Table 1
The summary of selected vegetation metrics/indices.

Metrics	Description	Unit, Range
Tree Cover (VC_Tree)	Proportion of landscape occupied by Tree	%; 0–100
Grass Cover (VC_Grass)	Proportion of landscape occupied by Grass	%; 0–100
Edge Density (ED)	Total perimeter of patches divided by total area of landscape	/ha; ≥0
Patch Density (PD)	Total number of patches divided by total area of landscape	/ha; > 0
Shape Index (SI)	Total patch perimeter divided by the square root of patch area, adjusted by a constant to adjust for a circular standard (Vector)	Non; > 1

non-linear models, including logarithmic, exponential, and quadratic. Nonlinear models were evaluated as vegetation effects on microclimates are often saturating (e.g. Yokohari et al., 2001). We also performed multiple regression analysis to evaluate how different vegetation factors influence urban heat in an integrated analysis. We selected all eight vegetation indices (four each for grass and tree cover) as independent variables and three LST indices as dependents, then we selected the stepwise method to filter the three most determinative variables to cooling effects in R version 3.4 (https://www.r-project.org). When choosing the best fitting model for relationships, models were evaluated and identified using the Akaike information criterion (AIC) (Akaike, 1974) where the smallest AIC value was chosen as the best statistical model. AIC was calculated as:

$$AIC = n[\ln(2\pi * RSS/n) + 1] + 2p \quad (1)$$

where RSS is the residual sum of squares between each model prediction and the observation, n is the number of observations and p is the total number of parameters in the model. In all cases, analyses were primarily directed to testing hypothesized controls of configuration to LST rather than generate predictive models.

4. Results

4.1. Vegetation cover reduces LST at all scales

Correlations between vegetation, both tree and grass cover, and LST indices were consistent and sensitive to all scales examined (Figs. 3 and 4; Supplemental Table 1). In addition, the magnitudes of tree cover ($r = -0.27$ to -0.68, mean $= -0.43$, $p < 0.05$) in cooling urban heat is greater than that of grass cover ($r = -0.25$ to -0.54, mean $= -0.33$, $p < 0.05$) (Supplemental Table 1), although substantial overlap in cooling capacity was observed and individual models had large uncertainties. Mean, Max, and Min LST were all negatively related to vegetation cover (except Max LST for tree cover at neighborhood level) (Fig. 3), and Mean LST showed the highest correlation for both vegetation types (Supplemental Table 1). Moreover, at the circular plot scale the greenspace had generally higher correlative coefficients ($r = -0.25$ to -0.68, mean $= -0.42$, $p < 0.05$) than at neighborhood scales ($r = -0.27$ to -0.57, mean $= -0.37$, $p < 0.05$), especially for mean temperature (mean $= -0.61$ vs -0.48) (Supplemental Table 1).

4.1.1. Cooling effects of tree cover at all scales

At the circular plot scale, tree cover was more correlated to LST indices than at the neighborhood scale (Fig. 3, Supplemental Fig. 1). For all different sizes of circular plots, tree cover was negatively related to Mean, Max and Min LST ($p < 0.05$), while the magnitudes differed among the three LST indices (Supplemental Table 1). Compared to other LST indices, Mean LST had stronger magnitudes of relationships with tree cover ranging from -0.55 to -0.62 ($p < 0.05$) across plot sizes. Correlations of Max LST and tree cover were consistently negative across circular plots (-0.35- -0.39, $p < 0.05$), while correlations between Min LST and tree cover decreased from -0.39 to -0.21 ($p < 0.05$). Although the correlations were generally negative across scales, the best fitting models differed among scales and LST indices (Fig. 3). Correlations between tree cover and LST were best predicted by linear models at the neighborhood scale. At the circular plot scale the relationships between tree cover and either Mean or Max LST were best represented as a linear function while a logarithmic function was the best model for the relationship between Min LST and tree cover.

4.1.2. Cooling effects of grass cover at all scales

Grass cover was negatively related with LST indices ($p < 0.05$). While the effect of grass cover was less than tree cover, the trends and scale-effects were similar to that of tree covers (Figs. 3 and 4). For instance, grass cover had stronger correlations with LST indices at plot scale than neighborhood scale for Mean LST (Supplemental Table 1) and the Min LST was best predicted by logarithmic function of grass cover at circular plot scale ($p < 0.05$). At the same time, correlations between grass cover and Max LST were observed at neighborhood scale while the correlations were insignificant for tree cover. Concerning the cooling effect magnitude at different plot sizes, similar to tree cover, Mean LST remained stable (-0.51 to -0.54, $p < 0.05$). However, the magnitudes of correlations decreased from -0.45 to -0.14 ($p < 0.05$) for Max LST; and -0.27 to -0.19 ($p < 0.05$) for Min LST, with the increase of plot size (Supplemental Table 1).

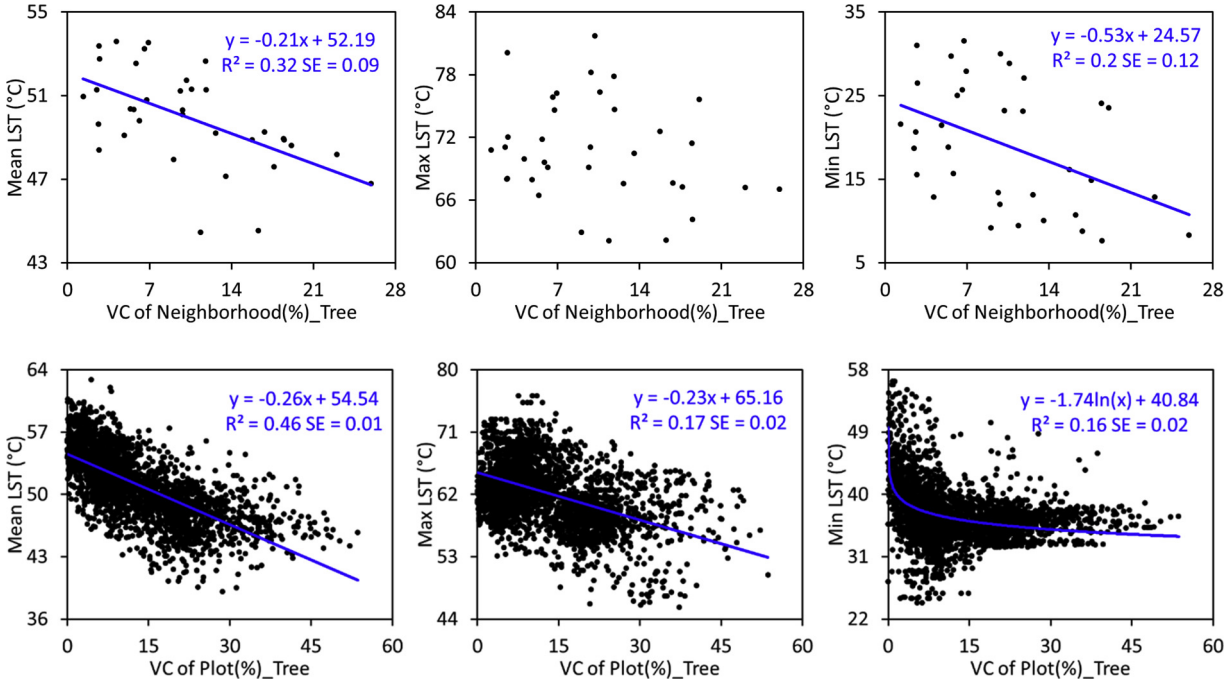

Fig. 3. The relationships between tree cover and LST for neighborhood and circular plot scales. *Lines indicate the correlation is significant at level of 0.05.*

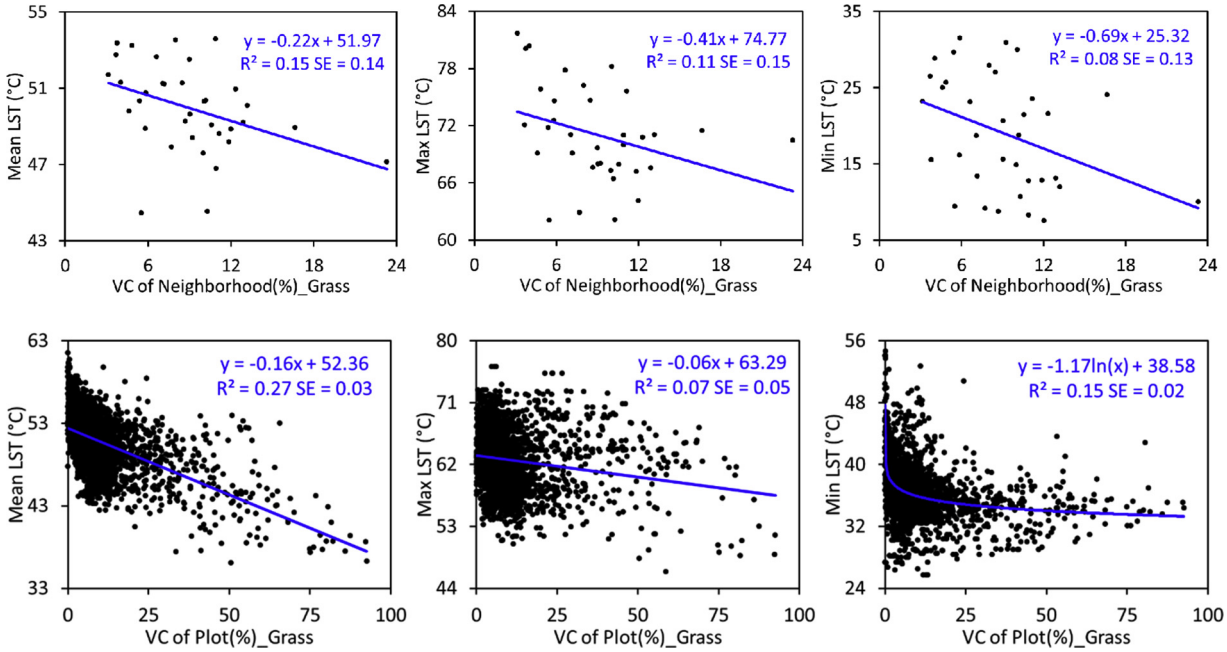

Fig. 4. The relationships between grass cover and LST for neighborhood and circular plot scales. Lines indicates the correlation is significant at level of 0.05.

4.2. Vegetation configuration affecting LST at all scales

Correlations between configuration metrics and LST indices depended on and dramatically varied among green types, configuration metrics, LST indices, and scales (Supplemental Fig. 1 and 2; Supplemental Table 2). Similar to vegetation cover, configuration of trees had stronger correlations with LST than grass at all scales and LST indices ($p < 0.05$). Mean LST for both tree and grass cover was the most strongly correlated LST index with configuration metrics. In contrast, while vegetation cover had stronger correlations at the plot scale, most configuration metrics had stronger correlations at the neighborhood scale (Supplemental Table 2). The magnitudes of vegetation configuration correlations varied in magnitude and direction depending on landscape metrics and LST indices, and the correlations alternately increased, decreased, or remained nearly constant corresponding to changing scales (Fig. 5; Supplemental Table 2). The variations of patch density and LST relations suggested the sensitivity of patch sizes for temperatures.

4.2.1. Landscape configuration of tree cover affects LST

All configuration metrics were negatively correlated to LST indices ($r = -0.11$ to -0.6, $p < 0.05$) except Max LST and patch density ($r = -0.05$) or shape index ($r = -0.1$) at plot scale. Correlations between configuration metrics and LST indices were stronger at the neighborhood scale than plot scale except Max LST of edge density (Supplemental Fig. 1; Supplemental Table 2). For different plot scales, all LST indices were negatively correlated with edge density and shape index ($r = -0.04$ to -0.6, $p < 0.05$ except shape index at smaller plots). With increasing circular plot sizes, the magnitude of correlations between configuration and LST increased. For shape index, all three LST indices had a peaked sensitivity to configuration at 250 m ($p < 0.05$), while edge density had the strongest correlations at 150 m for Mean LST and at 200 m for Max and Min LST ($p < 0.05$) (Fig. 5; Supplemental Table 2). The sensitivity to scale of correlations between shape index and LST were more unpredictable, especially at smaller scales (< 90 m), than that of edge density. Mean LST had stronger correlations with edge density while Min LST had stronger correlation with shape index. All LST indices were significantly correlated with edge density at all circular plots, but for shape index only Min LST was significant at all circular plot scales. In contrast, correlations between LST indices and patch density were more variable and exhibited not only a change in magnitude but also direction. At finer scales, smaller than 150 m, both Mean and Max LST were positively correlated with patch density but at larger scales the correlation switched to negative and significant. Min LST was negatively correlated with patch density but the correlations were insignificant at the smaller scales, consistent with Mean and Max LST where significant correlations emerged when the plot scale exceeded 150 m. (Supplemental Figs. 1 and 2; Supplemental Table 2).

4.2.2. Landscape configuration of grass cover and LST

Compared to trees, grass configuration metrics had weaker correlations ($r = -0.22$ to -0.43, $p < 0.05$) with LST indices (Supplemental Fig. 1 and 2; Supplemental Table 2). However, differing from the other metrics of grass and all metrics of trees, edge density of grass had better correlation at plot scale ($r = -0.43$, $p < 0.05$) than that of tree cover ($r = -0.33$, $p < 0.05$), and the trends reacting to increased plot size differed in directions: Mean LST remained stable, Max LST increased, and Min LST decreased (Fig. 5; Supplemental Table 2). The scale-dependent variation in patch density and shape index for grass are more unpredictable and dependent on scales, metrics and LST indices. Except the insignificant relationship with Min LST, Mean and Max LST indices were related to the patch density of grass, similar to trees, had negative ($r = -0.21$ to -0.33, $p < 0.05$) and increased correlations with the increasing plot sizes, while Min LST exhibited a negative to positive transition (Supplemental Table 2), which differed to that of tree cover. Correlations of shape index of grass and LST were only significant for Min LST. Circular plots scales between 150–200 m were the threshold that the correlation became significant for all LSTs compared to trees, which occurred at about 90–150 m.

4.3. Vegetation determinants of LST

Vegetation cover is the most prominent factor to reduce urban heat, decreasing LST by 0.11–0.27 °C with increase 1% of vegetation for Mean LST ($p < 0.05$) (Table 2). Considering the vegetation types, tree cover (-0.13 to -0.14 to -0.27, $p < 0.05$) was more influential than grass cover (-0.11 to -0.22, $p < 0.05$) in cooling for all LST indices. The selected three configuration indices all contributed to cooler LST, however, the contribution of vegetation configuration depended on LST

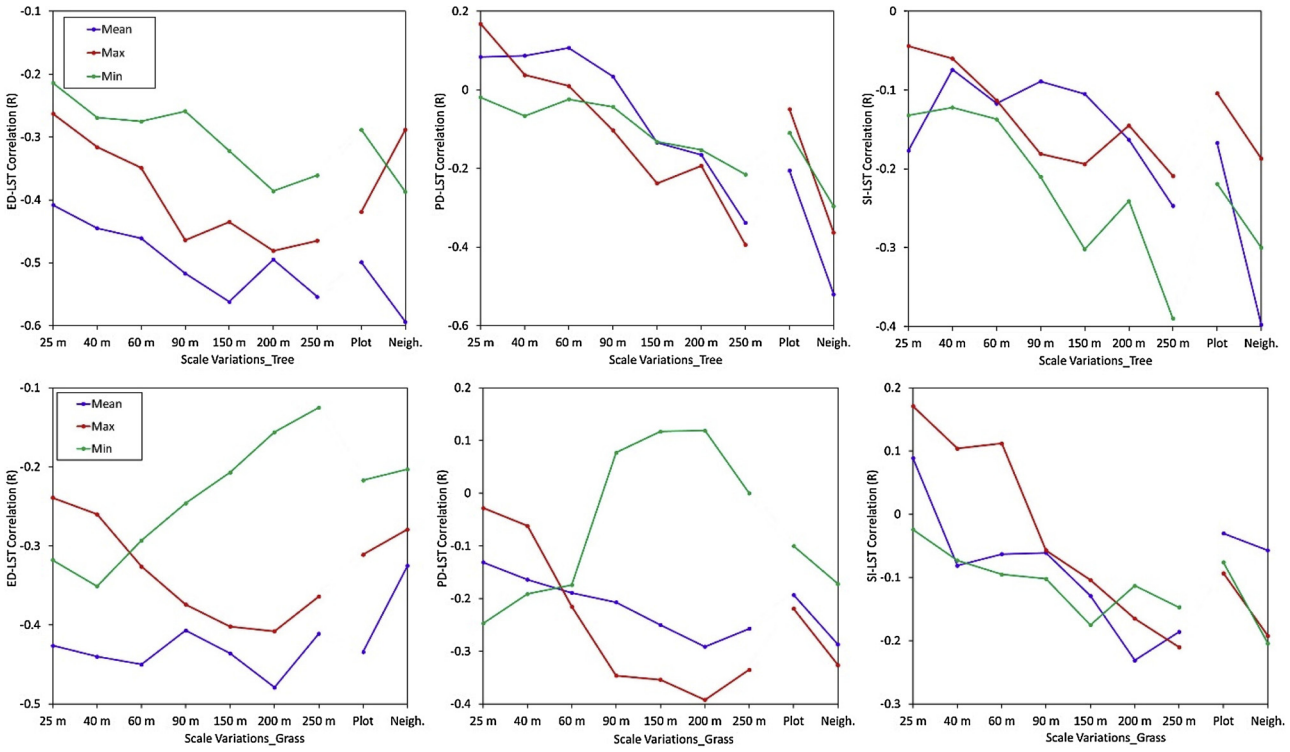

Fig. 5. Correlations between configuration metrics and LST for circular plot scales and entire neighborhood scale for three LST indices. *Neigh. is the whole neighborhood scale.*

indices and metrics (Supplemental Tables 3 and 4). Across scales, the proportional contribution of tree configuration was 45% that of tree cover (standardized coefficients). Vegetation cover, both tree cover and grass cover, and edge density (and shape index) were predictors of Mean LST, while tree cover and patch density and shape metrics were predictors of Max and Min LST. For the circular plots, vegetation covers were always the most important factors in cooling Mean LST at all plot sizes, although the importance of configuration metrics depended on plot sizes (Table 2). Four of seven plot sizes included edge density, and two included shape index. For Max and Min LST, the magnitudes of vegetation cover of cooling effects decreased, but were still the most important factors, and still configuration remained in the best fit model (Supplemental Tables 3 and 4).

4.4. LST distributions within individual vegetation patches

LST variation within an individual patch, extending from the surroundings and into the patch center, differed between trees and grass. The average LST of all tree patches were reduced proceeding from the surroundings to the interior of transects from 53.04 to 37.92 °C ($r = -0.99$, $p < 0.05$) for Max LST, and from 43.26 to 32.2 °C ($r = -0.89$, $p < 0.05$) for Mean LST, and from 33.25 to 32.24 °C

Table 2
Multiple regression analysis between configuration of vegetation metrics and Mean LST.

Scale	Variable	UC	SC	95% CI		Scale	Variable	UC	SC	95% CI	
25	VC_Grass	−0.13**	−0.52	−0.14	−0.11	40	VC_Tree	−0.16**	−0.51	−0.17	−0.15
	VC_Tree	−0.15**	−0.37	−0.18	−0.12		VC_Grass	−0.14**	−0.33	−0.17	−0.11
	SI_Tree	−0.43**	−0.15	−0.46	−0.41		ED_Grass	−0.07**	−0.17	−0.09	−0.05
	Constant	55.6		54.52	56.67		Constant	54.94		54.35	55.52
	Adjusted R^2	0.51**					Adjusted R^2	0.56**			
60	VC_Grass	−0.14**	−0.56	−0.16	−0.12	90	VC_Tree	−0.18**	−0.39	−0.24	−0.13
	VC_Tree	−0.14**	−0.38	−0.15	−0.12		VC_Grass	−0.13**	−0.28	−0.21	−0.05
	ED_Tree	−0.03**	−0.14	−0.05	0.01		PD_Tree	−0.04**	−0.13	−0.07	−0.01
	Constant	55.17		54.63	55.71		Constant	56.13		55.47	56.88
	Adjusted R^2	0.59**					Adjusted R^2	0.58**			
150	VC_Tree	−0.16**	−0.51	−0.18	−0.13	200	VC_Tree	−0.27**	−0.5	−0.28	−0.24
	VC_Grass	−0.17**	−0.35	−0.2	−0.15		VC_Grass	−0.22**	−0.35	−0.25	−0.19
	ED_Tree	−0.02**	−0.15	−0.04	−0.01		SI_Tree	−0.35**	−0.13	−0.39	−0.32
	Constant	56.99		56.25	57.73		Constant	57.77		56.86	58.68
	Adjusted R^2	0.57**					Adjusted R^2	0.61**			
250	VC_Tree	−0.19**	−0.54	−0.23	−0.15	Neigh.	VC_Tree	−0.18**	−0.52	−0.23	−0.14
	ED_Tree	−0.09**	−0.4	−0.12	−0.07		VC_Grass	−0.16**	−0.23	−0.19	−0.13
	VC_Grass	−0.11**	−0.13	−0.12	−0.1		ED_Tree	−0.04**	−0.21	−0.05	−0.03
	Constant	56.77		56.05	57.49		Constant	51.29		50.51	52.56
	Adjusted R^2	0.58**					Adjusted R^2	0.55**			

UC-Unstandardized Coefficient; SC-Standardized Coefficient; CI-Confidence Interval; Neigh. stands for neighborhood.
**$P \leq 0.01$ (Two-tailed).

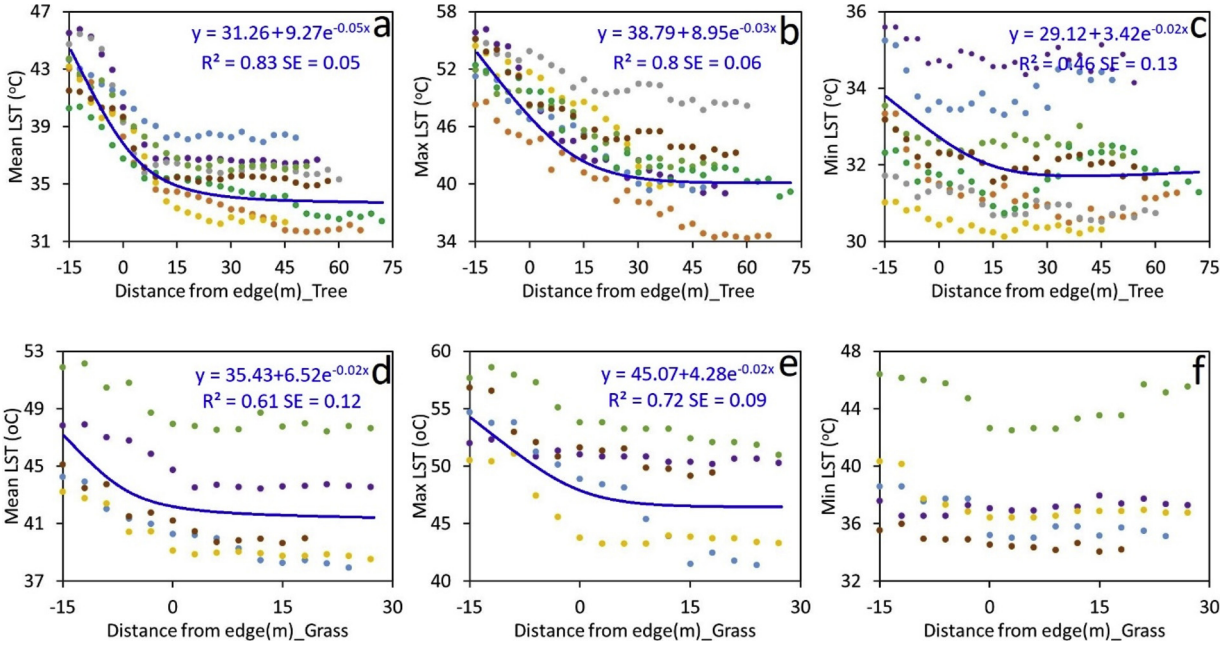

Fig. 6. Variations of LST within vegetation patches across transects from surroundings to patch edge to patch center. Dots with different color indicate different patches. *Lines indicate significant correlation ($p < 0.05$).*

($r = -0.61$, $p < 0.05$) for Min LST. The patches with longer distance from edge were cooler in the internal areas. Removing transects outside the patch, Mean ($r = -0.88$, $p < 0.05$) and Max LST ($r = -0.94$, $p < 0.05$) were still significantly related to the distance from patch edge (Fig. 6a,b). All transects followed an exponential relationship with differences among transects both for the exponential decay parameter and constant. For example, Mean LST of tree patches rapidly decreased within the first 20–30 m from patch edge (Fig. 6a). For Max LST, most patches exhibited rapid cooling at the first 30–40 m, and then decreased much slower, or even remained stable. For Min LST of tree patches, the LST variations fluctuated and most weren't significantly different between patch edge and interior of patch (0–75 m), except one patch, which showed an increase ($r = 0.24$, $p < 0.05$) (Fig. 6c).

For grass patches, Mean and Max LST were significantly ($p < 0.05$) related to the distance from surroundings to patch center. The most dramatic decreases occurred from outside the patch to the patch boundary (−15 to 0 m, $p < 0.05$) and the intra-patch LST variations from patch edge to center weren't significant for any LST indices for all grass patches examined (Fig. 6d–f). For each LST index, one patch showed different trends/variations from the other patches, blue dotted lines for Mean and Max LST (Fig. 6d–f). Without considering the specific patches, all LST indices were relatively constant or slightly changed across transects.

5. Discussion

High spatial resolution remotely sensed LST data sets provide unparalleled opportunities for quantifying vegetation-LST interactions at scales from individual patches to neighborhoods and allow new opportunities to identify the effects of vegetation configuration on microclimate distributions. With these data we found both tree and grass covers cooled LST with greater microclimate effects generated by tree cover. Nonetheless, vegetation configuration also significantly influenced LST from the neighborhood to individual patch scales. The effect of configuration exceeded 40% the effect of tree cover and was equivalent at many scales to grass cover. Given a certain amount of green cover, increasing vegetation edges and shape complexities were associated with cooler landscapes and would lead to warmer individual vegetation patches. The effects of configuration on LST were more influential at neighborhood scales than at plot scales. These findings were further corroborated by analyses of individual patch distributions and transects from outside to the center of vegetation patches. Together the results across neighborhoods, within neighborhoods, individual vegetation patches, and within patches support the hypothesis that effects of vegetation configuration on urban LST are associated with a combination of microclimate cooling within vegetation patches and energy exchanges between vegetation patches and surrounding environments. More edge length and complex boundaries strengthen energy exchanges between vegetation patches and surrounding environments while vegetation patches with more core area reduce energy exchanges with surrounding environments. With improved understanding of the biophysical underpinnings of how landscape configuration influences LST, improved urban designs can be achieved that look to maximize benefits for the same extent of vegetation coverage. Neighborhoods with a few larger and many smaller vegetation patches will likely provide benefits for whole landscape cooling while also providing locations of cool refugia accessible to residents.

5.1. Vegetation cover affects urban LST at multiple scales

Our multi-scale analysis with high resolution thermal data provide key support for previous work conducted at much larger resolution (Zhou et al., 2011; Li et al., 2013; Ren et al., 2015; Li et al., 2016) that vegetation cover is more prominent than configuration for urban cooling (Shashua-Bar and Hoffman, 2000). Trees can cool the environment, by providing shade and strengthening evapotranspiration rate and lower emissivity than built-up structures (Weng et al., 2004), as has been repeatedly shown (Sun and Chen, 2017; Zhang et al., 2017). For grass cover, shade is not a cooling factor; however, transpiration rates can contribute to surface cooling and depend on management and environmental conditions (Litvak and Pataki, 2016). Likely because of management and environmental differences, some previous studies suggested that grass can mitigate urban heat (Takebayashi and Moriyama, 2009; Skelhorn et al., 2014; Fan et al., 2015) and may in some cases even exceed cooling from trees (Wetherley et al. 2018), while some suggested the opposite (Heinl et al., 2015; Connors et al., 2013; Yang et al., 2017). In our analysis, cooling effects from grass cover were observed although these effects were limited compared to

trees (Figs. 3 and 4; Supplemental Table 1). However, grass cooling is still meaningful since grass and lawns comprise 70–75% of urban greenspace worldwide but the cooling effects are infrequently evaluated (Ignatieva et al., 2015; Wetherly et al. 2018). Uncertainties in the effect of vegetation cover on LST result from differences in other meteorological parameters, including wind speed and humidity, and may also be associated with effects of vegetation configuration.

5.2. Vegetation configuration affects urban LST at multi-scales

While vegetation cover was the most important factor for cooling urban LST, vegetation configuration was also related to LST distributions. Configuration metrics, including edge density, patch density and shape complexity were negatively correlated with LST, also consistent with previous studies (Li et al., 2013; Zhou et al., 2011). In contrast, the effects of patch density were more unpredictable. Although for smaller circular plots of tree cover and larger plots of grass cover, patch density had positive correlations with LST (Supplemental Table 2), which is also consistent with some previous analyses showing more fragmented landscapes led to cooler LST (Fan et al., 2015), while others suggested the opposite (Zhao et al., 2010). Our multiple-scale analysis may help resolve these inconsistencies as both directions of effects were observed in our analysis; for tree cover higher patch density increased Mean and Max LST indices at smaller scales while decreased these LST indices at neighborhood and larger plots (Supplemental Table 2). The variability of patch density influences on cooling indicted several configuration factors are synergetic. In the case of patch density, patch size is also a key variable; the same value of patch density may result from many different arrangements.

5.3. LST variation within individual patch

The variation of LST for individual vegetation patches from surroundings to patch center (Fig. 6) was consistent with predictions that configuration effects for more irregular vegetation patches are warmer. The LST variation within individual patches supported an energy exchange mechanism between patches as a key factor determining how landscape configuration influences urban LST. Vegetation edges reduced the temperature in the area immediately adjacent to the vegetation patches while also warming the vegetation at the edge compared to within the core. By increasing the patch size, the core area increases faster than the edge area, and vice versa (Didham and Lawton, 1999), explaining why larger patch sizes and more simple configurations would reduce patch LST. When the patch size is small enough, the entire patch becomes edge area (Wu and Vankat, 1991) where the patch-cooling was more limited although further distributed across the landscape. Conversely, since the temperature remained stable beyond a certain distance, increasing patch size beyond this threshold reduces vegetation LST because the core area is less affected by surroundings and more of core area remains cooler. This finding is consistent with nonlinear effects of greenspace cooling into residential areas previously observed (Yokohari et al., 2001). In addition, our LST variation analysis within tree patches suggested the critical patch size is achieved between 20–30 m from patch edge for Mean LST (Fig. 6a), and 30–40 m for Max LST (Fig. 6b). Therefore, a radius of 20–30 m at least for a tree patch is needed to cool surroundings and landscape when we assumed the patch is a regular circle shape, then the patch size is about 0.1–0.3 ha, for trees to result in enough core area to minimize the effects of adjacent patches. The critical patch size should be larger when the patch is shaped more irregularly. In the contrast, the landscape LST switched to an increase trend when patch size smaller than a critical size, as shown by the positive relationship between LST and patch density at fine plot scales (Supplemental Table 2). Therefore, the distribution patch size should be considered when increasing fragmentation of greenspace to increase edge- and shape-related features for landscape cooling.

5.4. Scale-dependence of vegetation configuration and LST relationships

An overarching finding of our work is the prominent influence of scale on urban LST distributions. At the endpoints of circular plot and whole neighborhood LST responded distinctly but systematically to vegetation: the influence of vegetation cover decreased, but influence of configuration increased with the increase of scale. These results contrast with previous studies relying on moderate resolution LST data (Saura, 2004; Saura and Martinez-Millan, 2001; Song et al., 2014; Wu, 2004; Zhou et al., 2017), which suggested vegetation density and configuration metrics were consistently responding to scales. We showed the correlation distinctly differed between vegetation cover, different configuration metrics, and LST indices across scales (Supplemental Table 2). Patch density was notable in scale dependence with LST where the correlation of patch density and Mean and Max LST changed from positive at smaller plots to negative at larger plots for tree covers. At the broader neighborhood scale, fragmented landscapes can increase vegetation edge length, cooling down surroundings and lead to a cooler landscape. However, when the plot decreased to less than 150 m (Supplemental Table 2), limited edge area of small patches existed for energy exchange to completely cool down surroundings, in these configurations both the landscape and vegetation LST can increase. The sensitivity of correlations, both in magnitude and direction, to changing scales demonstrates the importance of scale for evaluating vegetation cooling effects. Recognizing that changing scale leads to altered vegetation-LST correlations is important for evaluating the influence of landscape pattern on thermal environments (Zhang et al., 2013).

5.5. Implications and outlook in building climate resilient cities

With the wide spread findings of cooling benefits from urban trees, many cities are increasing urban vegetation density (Akbari and Konopacki, 2005; Rosenfeld et al., 1995; Taleghani et al., 2016). In looking to maximize the effectiveness of green infrastructure for urban cooling, the configuration of urban vegetation can substantially affect both landscape and local LST and the effectiveness of tree cover (Li et al., 2017; Zhou et al., 2011). In planning for vegetation arrangement, patch size and edge length can be key configuration variables influencing green infrastructure cooling capacity. Designing a landscape with many small tree patches can provide more landscape LST cooling than a single large one with the same total area of tree cover (Jiao et al., 2017). Increasing vegetation core area may also provide cooler refugia during high temperature periods. Taken together, arranging fewer large vegetation patches accessible to buildings or residents and many smaller vegetation patches will may help create more heat resilient cities. Linking the distributions of LST to other metrics of climate, including air temperature (Shiflett et al. 2017; Crum and Jenerette 2017), remains an important research challenge.

Acknowledgements

This research was supported by National Aeronautics and Space Administration (NASA) through grants NNX12AQ02G and NNX15AF36G, and National Science Foundation (NSF) through grant CBET-1444758.

Appendix A. Supplementary data

Supplementary material related to this article can be found, in the online version, at doi:https://doi.org/10.1016/j.agrformet.2019.107666.

References

Akaike, H., 1974. A new look at the statistical model identification. IEEE Trans. Automat.

Contr. 19, 716–723.
Akbari, H., Konopacki, S., 2005. Calculating energy-saving potentials of heat-island reduction strategies. Energy Policy 33, 721–756.
Baatz, M., Hoffmann, C., Willhauck, G., 2008. Progressing from object-based to object-oriented image analysis. In: Blaschke, T., Lang, S., Hay, G.J. (Eds.), Object-Based Image Analysis: Spatial Concepts for Knowledge-Driven Remote Sensing Applications. Springer, Berlin Heidelberg, pp. 29–42.
Benz, U.C., Hofmann, P., Willhauck, G., Lingenfelder, I., Heynen, M., 2004. Multi-resolution, object-oriented fuzzy analysis of remote sensing data for GIS-ready information. ISPRS J. Photogramm. Remote. Sens. 58, 239–258.
Bernstein, L.S., Adler-Golden, S.M., Sundberg, R.L., Levine, R.Y., Perkins, T.C., Berk, A., Ratkowski, A.J., Felde, G., Hoke, M.L., 2005. Validation of the quick atmospheric correction (QUAC) algorithm for VNIR-SWIR multi- and hyperspectral imagery. SPIE Proceedings, Algorithms and Technologies for Multispectral, Hyperspectral, and Ultraspectral Imagery XI. pp. 668–678.
Bowler, D.E., Buyung-Ali, L., Knight, T.M., Pullin, A.S., 2010. Urban greening to cool towns and cities: a systematic review of the empirical evidence. Landsc. Urban Plan. 97, 147–155.
Chen, A.L., Yao, L., Sun, R.H., Chen, L.D., 2014. How many metrics are required to identify the effects of the landscape pattern on land surface temperature? Ecol. Indic. 45, 424–433.
Chow, W.T.L., Brennan, D., Brazel, A.J., 2012. Urban heat island research in Phoenix, Arizona: theoretical contributions and policy applications. Bull. Am. Meteorol. Soc. 93, 517–530.
Connors, J.P., Galletti, C.S., Chow, W.T.L., 2012. Landscape configuration and urban heat island effects: Assessing the relationship between landscape characteristics and land surface temperature in Phoenix, Arizona. Landsc. Ecol. 28, 271–283.
Connors, J.P., Galletti, C.S., Chow, W.T.L., 2013. Landscape configuration and urban heat island effects: assessing the relationship between landscape characteristics and land surface temperature in Phoenix, Arizona. Landsc. Ecol. 28, 271–283.
Coutts, A.M., Harris, R.J., Phan, T., Livesley, S.J., Williams, N.S.G., Tapper, N.J., 2016. Thermal infrared remote sensing of urban heat: hotspots, vegetation, and an assessment of techniques for use in urban planning. Remote Sens. Environ. 186, 637–651.
Crum, S.M., Jenerette, G.D., 2017. Microclimate variation among urban land covers: The importance of vertical and horizontal structure in air and land surface temperature relationships. J. Appl. Meteorol. Climatol. 56, 2531–2543.
Deng, C., Wu, C., 2013. Examining the impacts of urban biophysical compositions on surface urban heat island: a spectral unmixing and thermal mixing approach. Remote Sens. Environ. 131, 262–274.
Didham, R.K., Lawton, J.H., 1999. Edge structure determines the magnitude of changes in microclimate and vegetation structure in tropical forest fragments. Biotropica 31, 17–30.
Fan, C., Myint, S.W., Zheng, B., 2015. Measuring the spatial arrangement of urban vegetation and its impacts on seasonal surface temperatures. Prog. Phys. Geogr. 39, 199–219.
Grimm, N.B., Redman, C.L., 2004. Approaches to the study of urban ecosystems: the case of Central Arizona-Phoenix. Urban Ecosyst. 7, 199–213.
Heinl, M., Hammerle, A., Tappeiner, U., Leitinger, G., 2015. Determinants of urban–rural land surface temperature differences – a landscape scale perspective. Landsc. Urban Plan. 134, 33–42.
Hook, S.J., Myers, J.J., Thome, K.J., Fitzgerald, M., Kahle, A.B., 2001. The MODIS/ASTER airborne simulator (MASTER)-A new instrument for earth science studies. Remote Sens. Environ. 76, 93–102.
Ignatieva, M., Ahrne, K., Wissman, J., Eriksson, T., Tidaker, P., Hedblom, M., Katterer, T., Marstorp, H., Berg, P., Bengtsson, J., 2015. Lawn as a cultural and ecological phenomenon: A conceptual framework for transdisciplinary research. Urban For. Urban Green. 14, 383–387.
Jenerette, G.D., 2018. Ecological contributions to human health in cities. Landsc. Ecol. 33, 1655–1668.
Jenerette, G.D., Harlan, S.L., Buyantuev, A., Stefanov, W.L., Declet-Barreto, J., Ruddell, B.L., Myint, S.W., Kaplan, S., Li, X., 2016. Micro scale urban surface temperatures are related to land cover features and heat related health impacts in Phoenix, AZ, USA. Landsc. Ecol. 31, 745–760.
Jenerette, G.D., Wu, J., 2001. Analysis and simulation of land-use change in the central Arizona, Phoenix region, USA. Landsc. Ecol. 16, 611–626.
Jiao, M., Zhou, W., Zheng, Z., Wang, J., Qian, Y., 2017. Patch size of trees affects its cooling effectiveness: a perspective from shading and transpiration processes. Agric. For. Meteorol. 247, 293–299.
Johnson, B.R., Young, S.J., 1998. In-scene atmospheric compensation: application to SEBASS data collected at the ARM site. The Aerospace Corporation.
Kealy, P.S., Hook, S.J., 1993. Separating temperature and emissivity in thermal infrared multispectral scanner data: implications for recovering land surface temperatures. IEEE Trans. Geosci. Remote. Sens. 31, 1155–1164.
Kong, F., Yin, H., James, P., Hutyra, L.R., He, H.S., 2014. Effects of spatial pattern of greenspace on urban cooling in a large metropolitan area of eastern China. Landsc. Urban Plan. 128, 35–47.
Köppen, W., 1884. The thermal zones of the earth according to the duration of hot, moderate and cold periods and to the impact of heat on the organic world. Meteorol. Z. 20, 351–360 (published 2011).
Laurance, W.F., Yensen, E., 1991. Predicting the impacts of edge effects in fragmented habitats. Biol. Conserv. 55, 77–92.
Li, X., Kamarianakis, Y., Ouyang, Y., Turner, B.L., Brazel, A., 2017. On the association between land system architecture and land surface temperatures: Evidence from a Desert Metropolis-Phoenix, Arizona, USA. Landsc. Urban Plan. 163, 107–120.
Li, X., Li, W., Middel, A., Harlan, S.L., Brazel, A.J., Turner, B.L., 2016. Remote sensing of the surface urban heat island and land architecture in Phoenix, Arizona: combined effects of land composition and configuration and cadastral–demographic–economic factors. Remote Sens. Environ. 174, 233–243.
Li, X., Myint, S.W., Zhang, Y., Galletti, C., Zhang, X., Turner, B.L., 2014. Object-based land-cover classification for metropolitan Phoenix, Arizona, using aerial photography. Int. J. Appl. Earth Obs. Geoinf. 33, 321–330.
Li, J.X., Song, C.H., Cao, L., Zhu, F.G., Meng, X.L., Wu, J.G., 2011. Impacts of landscape structure on surface urban heat islands: A case study of Shanghai, China. Remote Sens. Environ. 115, 3249–3263.
Li, X., Zhou, W., Ouyang, Z., 2013. Relationship between land surface temperature and spatial pattern of greenspace: what are the effects of spatial resolution? Landsc. Urban Plan. 114, 1–8.
Li, X., Zhou, W., Ouyang, Z., Xu, W., Zheng, H., 2012. Spatial pattern of greenspace affects land surface temperature: evidence from the heavily urbanized Beijing metropolitan area, China. Landsc. Ecol. 27, 887–898.
Leuzinger, S., Vogt, R., Korner, C., 2010. Tree surface temperature in an urban environment. Agric. For. Meteorol. 150, 56–62.
Litvak, E., Pataki, D.E., 2016. Evapotranspiration of urban lawns in a semi-arid environment: An in situ evaluation of microclimatic conditions and watering recommendations. J. Arid Environ. 134, 87–96.
Matlack, G.R., 1994. Vegetation dynamics of the forest edge-trends in space and successional time. J. Ecol. 82 (1), 113–123.
McDonald, R.I., Kroeger, T., Zhang, P., Hamel, P., 2019. The value of US urban tree cover for reducing heat-related health impacts and electricity consumption. Ecosystems. https://doi.org/10.1007/s10021-019-00395-5.
Myint, S.W., Zheng, B., Talen, E., Fan, C., Kaplan, S., Middel, A., Smith, M., Huang, H.-P., Brazel, A., 2015. Does the spatial arrangement of urban landscape matter? Examples of urban warming and cooling in Phoenix and Las Vegas. Ecosyst. Health Sustain. 1, 1–15.
Peng, J., Jia, J., Liu, Y., Li, H., Wu, J., 2018. Seasonal contrast of the dominant factors for spatial distribution of land surface temperature in urban areas. Remote Sens. Environ. 215, 255–267.
Rosenfeld, A.H., Akbari, H., Bretz, S., Fishman, B.L., Kurn, D.M., Sailor, D., Taha, H., 1995. Mitigation of urban heat islands: materials, utility programs, updates. Energy Build. 22, 255–265.
Ruddell, D., Hoffman, D., Ahmad, O., Brazel, A., 2013. Historical threshold temperatures for Phoenix (urban) and Gila Bend (desert), central Arizona, USA. Clim. Res. 55, 201–215.
Ren, P., Meng, Q.L., Zhang, Y.F., Zhao, L.H., Yuan, X., Feng, X.H., 2015. An unmanned airship thermal infrared remote sensing system for low-altitude and high spatial resolution monitoring of urban thermal environments: Integration and an experiment. Remote Sensing 7, 14259–14275.
Saura, S., 2004. Effects of remote sensor spatial resolution and data aggregation on selected fragmentation indices. Landsc. Ecol. 19, 197–209.
Saura, S., Martinez-Millan, J., 2001. Sensitivity of landscape pattern metrics to map spatial extent. Photogramm. Eng. Remote Sens. 67, 1027–1036.
Shashua-Bar, L., Hoffman, M.E., 2000. Vegetation as a climatic component in the design of an urban street - An empirical model for predicting the cooling effect of urban green areas with trees. Energy Buildings 31, 221–235.
Shiflett, S.A., Liang, L., Crum, S.M., Feyisa, G.L., Wang, J., Jenerette, G.D., 2017. Variation in the urban vegetation, surface temperature, air temperature nexus. Sci. Total Environ. 579, 495–505.
Skelhorn, C., Lindley, S., Levermore, G., 2014. The impact of vegetation types on air and surface temperatures in a temperate city: a fine scale assessment in Manchester, UK. Landsc. Urban Plan. 121, 129–140.
Song, J., Du, S., Feng, X., Guo, L., 2014. The relationships between landscape compositions and land surface temperature: quantifying their resolution sensitivity with spatial regression models. Landsc. Urban Plan. 123, 145–157.
Stone, B., Vargo, J., Habeeb, D., 2012. Managing climate change in cities: will climate action plans work? Landsc. Urban Plan. 107, 263–271.
Sun, R., Chen, L., 2017. Effects of green space dynamics on urban heat islands: Mitigation and diversification. Ecosyst. Serv. 23, 38–46.
Taleghani, M., Sailor, D., Ban-Weiss, G.A., 2016. Micrometeorological simulations to predict the impacts of heat mitigation strategies on pedestrian thermal comfort in a Los Angeles neighborhood. Environ. Res. Lett. 11.
Takebayashi, H., Moriyama, M., 2009. Study on the urban heat island mitigation effect achieved by converting to grass-covered parking. Sol. Energy 83, 1211–1223.
Tayyebi, A., Jenerette, G.D., 2016. Increases in the climate change adaption effectiveness and availability of vegetation across a coastal to desert climate gradient in metropolitan Los Angeles, CA, USA. Sci. Total Environ. 548–549, 60–71.
Tayyebi, A., Jenerette, G.D., 2018. Assessing diel urban climate dynamics using a land surface temperature harmonization model. Int. J. Remote Sens. 39, 3010–3028.
Weng, Q., 2009. Thermal infrared remote sensing for urban climate and environmental studies: methods, applications, and trends. ISPRS J. Photogramm. Remote. Sens. 64, 335–344.
Weng, Q., Liu, H., Liang, B., Lu, D., 2008. The spatial variations of urban land surface temperatures: pertinent factors, zoning effect, and seasonal variability. IEEE J. Sel. Top. Appl. Earth Obs. Remote. Sens. 1, 154–166.
Weng, Q., Lu, D., Schubring, J., 2004. Estimation of land surface temperature–vegetation abundance relationship for urban heat island studies. Remote Sens. Environ. 89, 467–483.
Weng, Q., Quattrochi, D.A., 2006. Thermal remote sensing of urban areas: an introduction to the special issue. Remote Sens. Environ. 104, 119–122.
Wetherley, E.B., McFadden, J.P., Roberts, D.A., 2018. Megacity-scale analysis of urban vegetation temperatures. Remote Sens. Environ. 213, 18–33.
Wu, J., 2004. Effects of changing scale on landscape pattern analysis: scaling relations. Landsc. Ecol. 19, 125–138.

Wu, J., Vankat, J.L., 1991. An area-based model of species richness dynamics of forest islands. Ecol. Modell. 58, 249–271.
Yan, J., Zhou, W., Han, L., Qian, Y., 2018. Mapping vegetation functional types in urban areas with WorldView-2 imagery: integrating object-based classification with phenology. Urban For. Urban Green. 31, 230–240.
Yang, C., He, X., Yu, L., Yang, J., Yan, F., Bu, K., Chang, L., Zhang, S., 2017. The cooling effect of urban parks and its monthly variations in a snow climate city. Remote Sens. 9, 1066.
Yokohari, M., Brown, R.D., Kato, Y., Yamamoto, S., 2001. The cooling effect of paddy fields on summertime air temperature in residential Tokyo, Japan. Landsc. Urban Plan. 53 (1-4), 17–27.
Zhang, Y., Odeh, I.O.A., Ramadan, E., 2013. Assessment of land surface temperature in relation to landscape metrics and fractional vegetation cover in an urban/peri-urban region using Landsat data. Int. J. Remote Sens. 34, 168–189.
Zhang, Y., Murray, A.T., Turner, B.L., 2017. Optimizing green space locations to reduce daytime and nighttime urban heat island effects in Phoenix, Arizona. Landsc. Urban Plan. 165, 162–171.
Zhang, X., Zhong, T., Feng, X., Ke Wang, K., 2009. Estimation of the relationship between vegetation patches and urban land surface temperature with remote sensing. Int. J. Remote Sens. 30, 2105–2118.
Zhao, X., Huang, J., Ye, H., Wang, K., Qiu, Q., 2010. Spatiotemporal changes of the urban heat island of a coastal city in the context of urbanisation. Int. J. Sustain. Dev. World Ecol. 17, 311–316.
Zhou, W., Huang, G., Cadenasso, M.L., 2011. Does spatial configuration matter? Understanding the effects of land cover pattern on land surface temperature in urban landscapes. Landsc. Urban Plan. 102, 54–63.
Zhou, W., Wang, J., Cadenasso, M.L., 2017. Effects of the spatial configuration of trees on urban heat mitigation: a comparative study. Remote Sens. Environ. 195, 1–12.